High-fidelity Greenberger-Horne-Zeilinger state generation within nearby nodes

Caprara Vivoli, Valentina; Ribeiro, Jérémy; Wehner, Stephanie

Important note
To cite this publication, please use the final published version (if applicable).
Please check the document version above.

High-fidelity Greenberger-Horne-Zeilinger state generation within nearby nodes

Valentina Caprara Vivoli,[*] Jérémy Ribeiro [⊙], and Stephanie Wehner

QuTech, Delft University of Technology, Lorentzweg 1, 2628 CJ Delft, The Netherlands

Generating entanglement in a distributed scenario is a fundamental task for implementing the quantum network of the future. We here report a protocol that uses only linear optics for generating Greenberger-Horne-Zeilinger states with high fidelities in a nearby node configuration. Moreover, we analytically show that the scheme is optimal for certain initial states in providing the highest success probability for sequential protocols. Finally, we give some estimates for the generation rate in a real scenario.

I. INTRODUCTION

Entanglement has revealed several interesting applications in quantum networks. For example, bipartite entanglement can be used for quantum cryptography tasks, i.e., quantum key distribution [1,2], teleportation [3], superdense coding [4], and bit commitment [5,6]. However, more and more interest has been recently shown in the study of multipartite entanglement. Several uses are nowadays known, such as reducing communication complexity [7,8] and distributed quantum computation [9–12]. Furthermore, there are multiple uses in quantum cryptography, namely quantum secret sharing [13], N-partite quantum key distribution, also known as conference key agreement [14], and anonymous transfer [15]. Multipartite entanglement could also be extremely useful for implementing quantum repeaters of second and third generation [16–19]. Finally, it has recently been pointed out that the use of multipartite entanglement could be fruitful for synchronizing several atomic clocks [20]. Greenberger-Horne-Zeilinger (GHZ) states [21] are particularly suitable for all these purposes. It is, thus, an interesting question how we can best generate such state in a distributed scenario, i.e., where the qubits between which the entanglement is shared can interact only through ancillary modes. In the case of two-qubit entanglement, there is already a protocol [22,23] (see Fig. 1), using ancillary photonic modes, that works pretty well for generating maximally entangled states in matter systems and low-loss regimes. However, it is still not very clear how this scheme can be extended in the case of multipartite entanglement.

In the latter case, there have been some proposals as well [24–28]. They all consist of two steps: (i) maximally entangled states are generated between two nodes through Bell measurements, and (ii) local probabilistic operations inside the nodes or additional Bell measurements are realized, generating multipartite entanglement all along the network. Concerning the network structure, it can vary from long chains of nodes to closed configurations with nearby nodes. Even though the first structure allows long distances to be covered, the second gives the possibility to make all the nodes interact with each other through a central station. So far, little effort has been put into the study of fidelity and generation rate, and for the most part without any study of the trade-off between these two quantities.

Remark. From now on we loosely use the term Bell measurement to refer to the measurement performed by interference of two optical modes on a beam splitter followed by two non-photon-number-resolving detectors, where the detection of a photon on one detector determines the success.

A. Setup and motivation

The goal of this work is to study optimal ways of generating N-partite GHZ states with very high fidelity. The setup that we have in mind is represented in Fig. 2. We want to generate a GHZ state between N quantum nodes, each constituted by a data qubit (subsystem A). To do so each node can send an ancillary qubit to a central node (central station) that can perform a measurement. We do not restrict our study to any specific measurement, except that it have a binary outcome, *success* or *failure*, and thus the measurement is modeled by a positive-operator valued measurement (POVM). When the outcome is labeled as *success* it means that a GHZ state has been generated between the N nodes. When the outcome is labeled as a failure, no GHZ state has been generated. Restricting ourselves to binary outcomes reduces in a realistic setting the number of steps, operations, waiting times, and thus noise. As a result, the fidelity of the final state is expected to be high. In this article we are going to answer the following three questions.

(i) Constraining the final fidelity to be $F = 1$, what is the highest probability of success p_{succ}? And what is the POVM that corresponds to such p_{succ}?

(ii) Is there a simple way to experimentally implement the POVM achieving the maximal p_{succ}?

(iii) What is the rate that we can expect from such implementation in a realistic scenario?

B. Results and structure of the article

The article addresses and answers all three questions of the previous section. Each question is answered in a separate section.
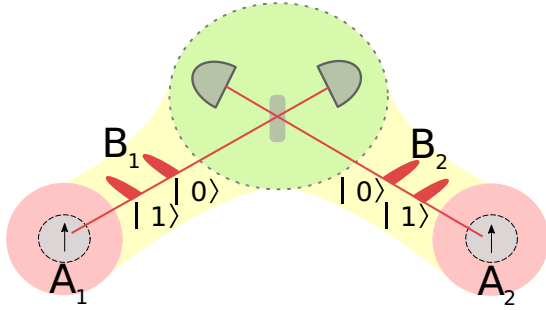
―――――
[*]capraravalentina@gmail.com

FIG. 1. Barrett-Kok scheme [22,23]. Two nodes constituted by two-level systems are optically excited so that they generate matter-photon entanglement, i.e., $(|00\rangle + |11\rangle)_{A_j B_j}$. The photons are sent to a common station where a partial Bell measurement, which can distinguish only two Bell states, is performed.

(i) In Sec. II, we work in a noise free model, where we first show an upper-bound on the product $F p_{\text{succ}}$ as a function of the initial state, where F is the fidelity between the N-partite GHZ state and the final state conditioned on *success*, and p_{succ} is the success probability. We then explicitly show that there exists a binary POVM that saturates the upper bound for $F p_{\text{succ}}$. Finally we search for initial states that allow us to get a fidelity of $F = 1$ between the final output state and the GHZ state. We conclude that there exists a measurement (determined by the projector onto the N-partite GHZ state) that allows for the creation of an N-partite GHZ state with an optimal success probability of 2^{-N}.

(ii) In Sec. III, we show how to implement the abovementioned optimal POVM with only linear optics and non-photon-resolving detectors (see Fig. 5). It turns out that to perform this measurement we only need measurements between each two consecutive nodes. It means that a "central station" is not
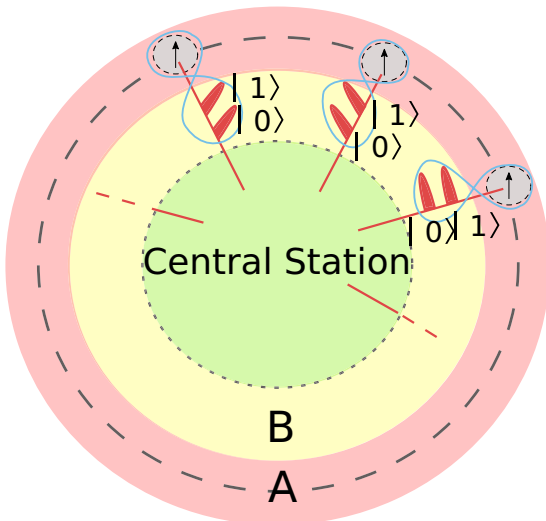
needed. This allows for more flexibility in the implementation of the measurement, which can be used to reduce losses and other sources of noise. This implementation is inspired by an old work [29] in all photonic systems, and we show that it is a natural extension of the scheme proposed in Refs. [22,23].

(iii) Finally in Sec. IV, we give some results in a scenario that could be reasonable in the near future. We focus on the entanglement generation rate, comparing it for different numbers of nodes and internode distance.

II. NODES-CENTER SCENARIO

In this section we first show that there is an upper bound for the product of the fidelity (F) between the GHZ state and the final state and the success probability (p_{succ}) of the POVM, depending on the initial state. Second, we derive the map that allows the upper bound to be reached and we show that only for $p_{\text{succ}} = 2^{-N}$ is it possible to saturate the upper bound and get $F = 1$. In order to do so, let us consider the scenario represented in Fig. 2. The total system is composed of two subsystems, A and B, each one composed of N qubits. We take the initial state to be

$$|\Psi_{\text{in}}\rangle_{AB} = \bigotimes_{j=1}^{N} (\sqrt{1-\epsilon}|00\rangle + \sqrt{\epsilon}|11\rangle)_{A_j B_j}, \qquad (1)$$

where A_j (B_j) are qubits, and $0 \leqslant \epsilon \leqslant 1$. We assume that in the central station it is possible to perform an arbitrary POVM.

A. Optimal $F p_{\text{succ}}$

Our goal, here, is to derive an upper-bound for $F p_{\text{succ}} = \text{Tr}[(|\text{GHZ}\rangle\langle\text{GHZ}|_A \otimes \Pi_B^{\text{succ}})|\Psi_{\text{in}}\rangle\langle\Psi_{\text{in}}|_{AB}]$, when optimizing our POVM elements Π_B^{succ} on B indicating successful generation. Let us consider the following series of inequalities,

$$
\begin{aligned}
F p_{\text{succ}} &\leqslant F p_{\text{succ}} + F_{\text{fail}} p_{\text{fail}} \\
&= \text{Tr}(|\text{GHZ}\rangle\langle\text{GHZ}|_A \otimes \Pi_B^{\text{succ}}|\Psi_{\text{in}}\rangle\langle\Psi_{\text{in}}|_{AB}) \\
&\quad + \text{Tr}[|\text{GHZ}\rangle\langle\text{GHZ}|_A \otimes (\mathbb{1} - \Pi^{\text{succ}})_B|\Psi_{\text{in}}\rangle\langle\Psi_{\text{in}}|_{AB}] \\
&= F[\text{Tr}_B(|\Psi_{\text{in}}\rangle\langle\Psi_{\text{in}}|_{AB}), |\text{GHZ}\rangle_A] \\
&= \tfrac{1}{2}[(1-\epsilon)^N + \epsilon^N]. \qquad (2)
\end{aligned}
$$

Here, p_{fail} is the probability that the measurement does not succeed, and F_{fail} is the overlap between the GHZ state and the state that would result from the fail outcome. $F[\text{Tr}_B(|\Psi_{\text{in}}\rangle\langle\Psi_{\text{in}}|_{AB}), |\text{GHZ}\rangle_A] = F(\Psi_{\text{in}}^A; \text{GHZ})$ is the fidelity between the initial state in A and the GHZ state. The previous upper bound can be interpreted saying that the maximal amount of entanglement that can be extracted from subsystem A does not depend on subsystem B. In the case when several success events are considered, the proof follows the same procedure for upper bounding the sum $\sum_i F^i p_{\text{succ}}^i$. One finds a sum of terms of the same form of the one of the fourth line of Eq. (2), where instead of the GHZ state there are several different GHZ-like states.

FIG. 2. Nodes-center scenario. The entire system is composed of two subsystems: A (pink shell) and B (yellow shell). Each subsystem is composed of N qubits. The qubits between A and B are entangled in pairs; i.e., there are N entangled pairs $(\sqrt{1-\epsilon}|00\rangle + \sqrt{\epsilon}|11\rangle)_{A_j B_j}$. The N qubits of subsystem B are analyzed together through a POVM in a central station.

B. Optimal map $\Pi_B^{\text{succ, opt}}$

For very small ϵ, the bound in Eq. (2) is close to $\frac{1}{2}$. We now ask (i) whether this upper bound is attainable and (ii) what is the maximal fidelity in this case?

In order to answer to these questions, it is necessary to find the POVM that allows us to reach $F(\Psi_{\text{in}}^A; \text{GHZ})$. Suppose that the bound (2) is attainable by $F^{\text{opt}} p_{\text{succ}}^{\text{opt}}$ and we look for the element $\Pi_B^{\text{succ, opt}}$ of a POVM such that

$$p_{\text{succ}}^{\text{opt}} = \text{Tr}_B \left[\Pi_B^{\text{succ, opt}}[(1-\epsilon)|0\rangle\langle 0| + \epsilon|1\rangle\langle 1|]_B^{\otimes N} \right] \quad (3)$$

is minimal and, hence, F^{opt} is maximal. $\Pi_B^{\text{succ, opt}}$ can be written as a $2^N \times 2^N$ square matrix of elements e_{lm}. One has, then,

$$p_{\text{succ}}^{\text{opt}} = e_{11}(1-\epsilon)^N + e_{2^N 2^N}\epsilon^N \quad (4)$$

and

$$F^{\text{opt}} p_{\text{succ}}^{\text{opt}} = \frac{1}{2}[e_{11}(1-\epsilon)^N + e_{2^N 2^N}\epsilon^N$$
$$+ (e_{12^N} + e_{2^N 1})\sqrt{\epsilon(1-\epsilon)}^N]$$
$$= \frac{1}{2}\left[p_{\text{succ}}^{\text{opt}} + (e_{12^N} + e_{2^N 1})\sqrt{\epsilon(1-\epsilon)}^N\right]. \quad (5)$$

The minimization of $p_{\text{succ}}^{\text{opt}}$ is subjected to five conditions. The first condition derives from the bound (2), i.e.,

(i)

$$F^{\text{opt}} p_{\text{succ}}^{\text{opt}} = \frac{1}{2} \text{Tr}_B \left[\Pi_B^{\text{succ, opt}}(\sqrt{1-\epsilon}^N|0\rangle^{\otimes N} + \sqrt{\epsilon}^N|1\rangle^{\otimes N}) \right.$$
$$\left. \times (\sqrt{1-\epsilon}^N\langle 0|^{\otimes N} + \sqrt{\epsilon}^N\langle 1|^{\otimes N})_B \right]$$
$$= \frac{1}{2}[(1-\epsilon)^N + \epsilon^N].$$

From the fact that $\Pi_B^{\text{succ, opt}}$ is an element of a POVM, we can derive the condition $0 \leqslant \Pi_B^{\text{succ, opt}} \leqslant \mathbb{1}$. This leads us to the following four necessary conditions:

(ii) $0 \leqslant e_{11} \leqslant 1$,
(iii) $0 \leqslant e_{2^N 2^N} \leqslant 1$,
(iv) $e_{12^N} = e_{2^N 1}^*$,
(v) $e_{12^N} e_{2^N 1} \leqslant \min[e_{11}e_{2^N 2^N}, (1-e_{11})(1-e_{2^N 2^N})]$.

All the elements e_{lm} with $l, m \neq 1, 2^N$ do not influence the values of Eqs. (5) and (4). Hence, they can just be ignored. In order to keep Eq. (5) constant to the optimal value while we minimize $p_{\text{succ}}^{\text{opt}}$, e_{12^N} and $e_{2^N 1}$ must be real and, thus, equal [see conditions (iv) and (v)]. Hence,

$$F^{\text{opt}} p_{\text{succ}}^{\text{opt}} = \frac{1}{2}\left[p_{\text{succ}}^{\text{opt}} + 2e_{12^N}\sqrt{\epsilon(1-\epsilon)}^N\right]. \quad (6)$$

From condition (v), $e_{12^N}^2$ is maximal when it reaches the maximum of $\min[e_{11}e_{2^N 2^N}, (1-e_{11})(1-e_{2^N 2^N})]$, that is, when $e_{11}e_{2^N 2^N} = (1-e_{11})(1-e_{2^N 2^N})$. From this, it follows that $e_{11} + e_{2^N 2^N} = 1$ and $e_{12^N} = \sqrt{e_{11}e_{2^N 2^N}}$. Putting Eq. (6) equal to $\frac{1}{2}[(1-\epsilon)^N + \epsilon^N]$, one gets the final form of $\Pi_B^{\text{succ, opt}}$, i.e.,

$$\Pi_B^{\text{succ, opt}} = \begin{pmatrix} \frac{(1-\epsilon)^N}{(1-\epsilon)^N+\epsilon^N} & 0 & \cdots & 0 & \frac{\sqrt{\epsilon(1-\epsilon)}^N}{(1-\epsilon)^N+\epsilon^N} \\ 0 & & & & 0 \\ \vdots & & 0 & & \vdots \\ 0 & & & & 0 \\ \frac{\sqrt{\epsilon(1-\epsilon)}^N}{(1-\epsilon)^N+\epsilon^N} & 0 & \cdots & 0 & \frac{\epsilon^N}{(1-\epsilon)^N+\epsilon^N} \end{pmatrix}.$$
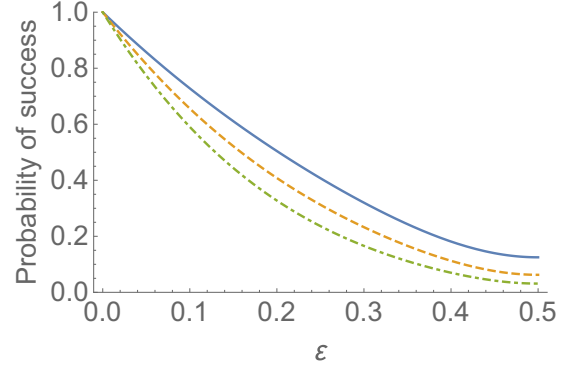$$(7)$$

FIG. 3. Optimal success probability. The optimal success probability $p_{\text{succ}}^{\text{opt}}$ is plotted as a function of ϵ in the [0,0.5] range for $N = 3$, 4, and 5 (solid, dashed, and dot-dashed curves, respectively). The function assumes values from 1 to $\frac{1}{2^N}$. The function goes from 1, when no operation is performed over system B, to $\frac{1}{2^N}$, when a perfect GHZ projector is performed.

For this POVM the probability of success is

$$p_{\text{succ}}^{\text{opt}} = \frac{(1-\epsilon)^{2N} + \epsilon^{2N}}{(1-\epsilon)^N + \epsilon^N}, \quad (8)$$

and the fidelity is

$$F^{\text{opt}} = \frac{1}{2}\frac{[(1-\epsilon)^N + \epsilon^N]^2}{(1-\epsilon)^{2N} + \epsilon^{2N}}. \quad (9)$$

Note that $\Pi_B^{\text{succ}} = \mathbb{1}$ always retrieves the bound of Eq. (2), with $p_{\text{succ}} = 1$ and $F = \frac{1}{2}[(1-\epsilon)^N + \epsilon^N]$. Thus, the POVM $\Pi_B^{\text{succ}} = w\Pi_B^{\text{succ, opt}} + (1-w)\mathbb{1}$, i.e., an interpolation between the optimal measurement and the identity, spans the threshold for all values of F and p_{succ} that optimize $F p_{\text{succ}}$.

Equation (8) is the optimal success probability as a function of ϵ and N when the bound of Eq. (2) is attained and F is maximal. Let us analyze Eqs. (8) and (9). The two functions are plotted as a function of ϵ for 3, 4, and 5 nodes in Figs. 3 and 4, respectively. Concerning the fidelity, it reaches the value 1 only for $\epsilon = \frac{1}{2}$, i.e., for an initial maximally entangled
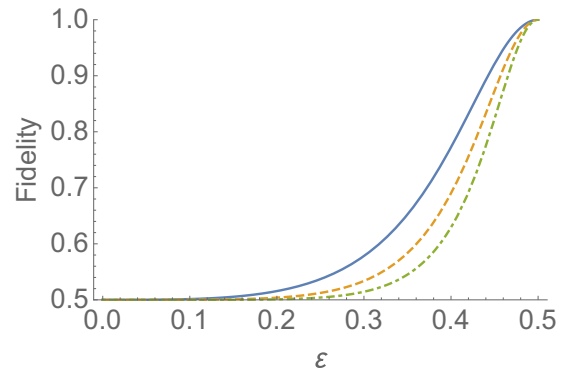

FIG. 4. Optimal fidelity. The optimal fidelity F^{opt} is plotted as a function of ϵ for $N = 3$, 4, and 5 (solid, dashed, and dot-dashed curves, respectively). Since the function is symmetrical with respect to $\epsilon = 0.5$, the plot is represented only in the [0,0.5] range. The function goes from 0.5, when no entanglement is generated, to 1, when the final state is the maximal entangled $|\text{GHZ}\rangle$.

state. For other values of ϵ, F^{opt} is always smaller than 1. The maximal success probability is obtained for $\epsilon = 0$. However, in this last case, the final state is $|0\rangle\langle 0|_A^{\otimes N}$ and $F = \frac{1}{2}$, which is clearly an uninteresting case since we are interested in high-fidelity GHZ generation. We can then conclude that the optimal case is $\epsilon = \frac{1}{2}$. $\Pi_B^{\text{succ, opt}}$ reduces to a $|\text{GHZ}\rangle$ projector.

III. OPTICAL GHZ PROJECTOR

In this section we present a possible way of implementing a $|\text{GHZ}\rangle$ projector. The envisioned setup is represented in Figs. 5(a) and 5(b). Subsystem A is the actual quantum network, composed of N nodes. Each node is constituted of a quantum system with two long-lived spin states [30–33], here called $|0\rangle$ and $|1\rangle$, that can be independently excited
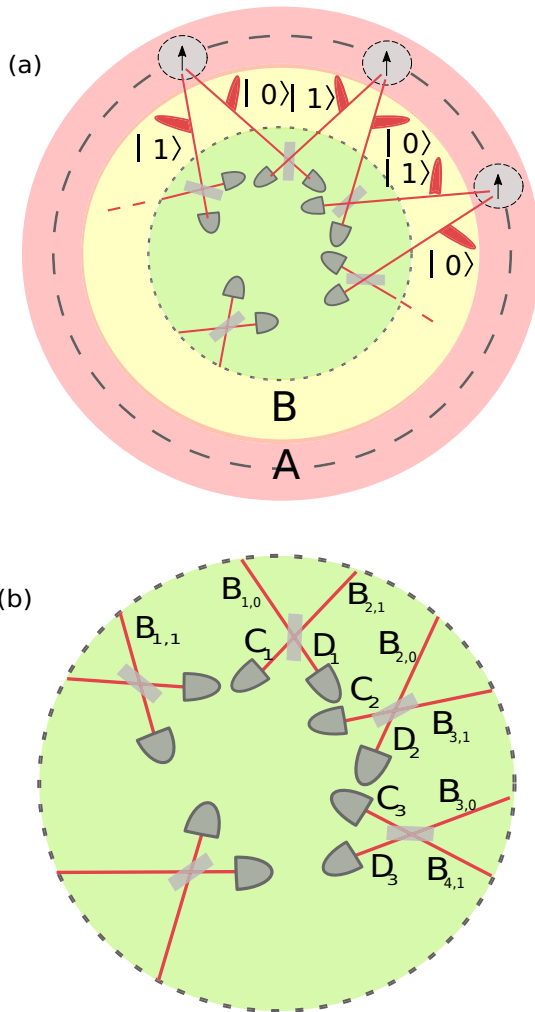

FIG. 5. Optical realization of a GHZ projector. (a) Entire setup. Subsystem A (pink shell) is composed of N spin qubits on the external circle. The spin qubits are excited so that they generate the state $|\Phi^+\rangle_{AB}$ between them and N photonic qubits, composing subsystem B (yellow shell). Each photonic qubit is converted in an optical-path qubit through an optical switch and sent to the central station [green (center) circle] where the projector is applied. (b) Central station. Two optical-path modes coming from two neighboring matter qubits impinge on the same beam splitter. A Bell measurement is performed on the C and D modes coming out from each beam splitter.

through optical pulses. As a consequence, each node is able to generate a maximally entangled spin-photon pair, i.e., $\frac{1}{\sqrt{2}}(|00\rangle + |11\rangle)_{A_j B_j}$, where $|0\rangle_{B_j}$ ($|1\rangle_{B_j}$) is a photon in the 0 (1) mode. The nodes interact with each other through the photonic 0-1 modes regrouped in subsystem B. The degree of freedom of modes in subsystem B depends on the nature of the nodes. For example, for nitrogen-vacancy (NV) centers [30,31] and trapped ions [32], the photonic qubits can be encoded in time-bin, and polarization, respectively.

The jth 0 and 1 modes are converted into two different spatial modes, $B_{j,0}$ and $B_{j,1}$, respectively. This can be done through an optical switch [34], with both modes directed to the central station [Fig. 5(b)] where Bell measurements between modes $B_{j,0}$ and $B_{j+1,1}$ are performed. In order to close the series of Bell measurements, a Bell measurement is performed between modes $B_{1,1}$ and $B_{N,0}$.

Proof. In this subsection, we prove that, depending on which set of detectors click, the setup in Fig. 5 allows us to generate two GHZ-like states on subsystem A. Moreover, we derive the success probability as a function of the losses and we show that, in the ideal case, each one of the final states has a probability of success 2^{-N}, equivalent to the one one would get for a GHZ projector. We split the proof into three steps. In step 1, we focus on one successful combination of clicks among the 2^N successful combinations. We prove that the event corresponding to this particular combination of clicks happens with probability $P_{\text{succ}} = \frac{2}{2^{2N}}\eta^N$, where η is the total probability that a photon does not get lost in the transmission and detected by a detector, and that a GHZ-like state is, thus, produced in A. In step 2, we show that all the other successful detector combinations project system A into a GHZ-like state with the same probability P_{succ}. In step 3, we show that the set of GHZ-like states that are generated is composed by only two states that differ by a relative phase. We calculate the total success probability for each GHZ-like state and show that it is equal to $P_{\text{succ}}^{\text{Tot}} = (\frac{\eta}{2})^N$. For no losses, 2^{-N} is the success probability that a GHZ projector $|\text{GHZ}\rangle\langle\text{GHZ}|_B$ would project system A into a $|\text{GHZ}\rangle_A$ state.

The total state $|\Phi^+\rangle_{AB}$ generated between subsystems A and B can be written in terms of creation operators as

$$|\Phi^+\rangle_{AB} = \frac{1}{\sqrt{2}^N}\Pi_{j=1}^N(a_{j,0}^\dagger b_{j,0}^\dagger + a_{j,1}^\dagger b_{j,1}^\dagger)|\mathbf{0}\rangle, \quad (10)$$

where $|\mathbf{0}\rangle$ is the vacuum, $a_{j,k}^\dagger$ is the creation operator of the $|k\rangle_{A_j}$ state on the jth spin qubit, and $b_{j,k}^\dagger$ is the jth creation operator of the photonic mode $|k\rangle_{B_j}$. Each photonic mode $B_{j,k}$ is converted into a sum of modes C_m and D_m when it impinges on a beam splitter. The equations that transform the operators $b_{j,k}^\dagger$ are $b_{j,0}^\dagger = \frac{1}{\sqrt{2}}(ic_j^\dagger + d_j^\dagger)$ and $b_{j,1}^\dagger = \frac{1}{\sqrt{2}}(c_{j-1}^\dagger + id_{j-1}^\dagger)$.

Hence, the state becomes $|\Psi\rangle_{ACD}$, i.e.,

$$|\Psi\rangle_{ACD} = \frac{1}{2^N}\Pi_{j=1}^N[a_{j,0}^\dagger(ic_j^\dagger + d_j^\dagger) + a_{j,1}^\dagger(c_{j-1}^\dagger + id_{j-1}^\dagger)]|\mathbf{0}\rangle. \quad (11)$$

Step 1. Let us first focus on one single successful combination of detections, which is when we get a detection on all detectors on modes C and none on modes D. The total detectors operator, composed of the no-click (click) operator

D_{nc}^D (D_{c}^C) on modes D (C), is $D_{\mathrm{nc}}^D D_{\mathrm{c}}^C = \Pi_{j=1}^N (1-\eta)^{d_j^\dagger d_j}[\mathbb{1} - (1-\eta)^{c_j^\dagger c_j}]$ [35]. Let us analyze this operator in more detail. Let us consider first the click operator on a single mode C_j, $D_{\mathrm{c}}^{C_j} = \mathbb{1} - (1-\eta)^{c_j^\dagger c_j} = \sum_{n=1}^{+\infty}[1-(1-\eta)^n]|n\rangle\langle n|_{C_j}$, where $|n\rangle_{C_j}$ is a Fock state of n photons. The effect of the operator $c_j^\dagger$ applied l times on the right side of $D_{\mathrm{c}}^{C_j}$ is

$$D_{\mathrm{c}}^{C_j} c_j^{\dagger l} = \sum_{n=l}^{+\infty}[1-(1-\eta)^n]\sqrt{\frac{n!}{(n-l)!}}|n\rangle\langle n-l|. \quad (12)$$

Note that in the previous equation if $l = 0$ there is no term in the sum with $\langle 0|_{C_j}$. The previous remark implies that, in order to have a detection in mode C_j, there must be at least a $c_j^\dagger$ in the detected state; i.e., there must be at least one photon in mode C_j. Let us consider, now, the operator $D_{\mathrm{nc}}^{D_j} = (1-\eta)^{d_j^\dagger d_j} = \sum_{n=0}^{+\infty}(1-\eta)^n|n\rangle\langle n|_{D_j}$. In this case, if there are no losses, the application of several $d_j^\dagger$ gives a success only with no photon on mode D_j; i.e., there are no $d_j^\dagger$ in the detected state. If losses occur, then there is a non-null probability of not having any detection in mode D_j and, as a consequence, a successful Bell measurement. Let us come back to the protocol. The N modes generate a photon each. We need N detections, each one in one of the N C modes. This implies two things. First, the only states that have successful outcomes do not have photons in any mode D; i.e., they do not have any one of the operators $d_j^\dagger$s. Second, in each mode C there is only one photon; i.e., in the final state each $c_j^\dagger$ appears only once. We can, now, continue the calculations. We have

$$\mathrm{Tr}_{CD}\left(|\Psi\rangle\langle\Psi|_{ACD}D_{\mathrm{nc}}^D D_{\mathrm{c}}^C\right)$$
$$= \frac{1}{2^{2N}}\mathrm{Tr}_C\left\{\Pi_{j=1}^N[\mathbb{1}-(1-\eta)^{c_j^\dagger c_j}]\right.$$
$$\times \Pi_{j=1}^N(ia_{j,0}^\dagger c_j^\dagger + a_{j,1}^\dagger c_{j-1}^\dagger)|\mathbf{0}\rangle\langle\mathbf{0}|$$
$$\left.\times \Pi_{j=1}^N(-ia_{j,0}c_j + a_{j,1}c_{j-1})\right\}$$
$$= \left(\frac{\eta}{2^2}\right)^N\left(\Pi_{j=1}^N ia_{j,0}^\dagger + \Pi_{j=1}^N a_{j,1}^\dagger\right)|\mathbf{0}\rangle\langle\mathbf{0}|$$
$$\times \left[\Pi_{j=1}^N(-i)a_{j,0} + \Pi_{j=1}^N a_{j,1}\right]$$
$$= \left(\frac{\eta}{2^2}\right)^N(i^N|0\rangle^N + |1\rangle^N)[(-i)^N\langle 0|^{\otimes N} + \langle 1|^{\otimes N}]_A$$
$$= 2\left(\frac{\eta}{2^2}\right)^N|\text{GHZ-like}\rangle\langle\text{GHZ-like}|_A. \quad (13)$$

The prefactor in front of $|\text{GHZ-like}\rangle\langle\text{GHZ-like}|_A$ in the last passage is the success probability of the set of Bell measurements $P_{\mathrm{succ}} = \eta^N 2^{1-2N}$. Hence, the final state is

$$|\text{GHZ-like}\rangle_A = \frac{1}{\sqrt{2}}(i^N|0\rangle^{\otimes N} + |1\rangle^{\otimes N})_A, \quad (14)$$

which is a GHZ state except for a phase factor that can be easily corrected.

Step 2. There are other $2^N - 1$ detector configurations that result in the success of the set of Bell measurements. If we choose other click-no click configurations, we have to invert the creation and annihilation operators for all modes where the success Bell measurement combination has been changed,

i.e., $d_m^{(\dagger)} \leftrightarrow c_m^{(\dagger)}$. It follows that the final states $|\Psi_{\mathrm{final}}\rangle_A$ are of the same form, i.e.,

$$|\Psi_{\mathrm{final}}\rangle_A = \frac{1}{\sqrt{2}}(i^k|0\rangle^{\otimes N} + i^l|1\rangle^{\otimes N})_A, \quad (15)$$

but the relative phase between $|0\rangle^{\otimes N}$ and $|1\rangle^{\otimes N}$ can change and depends on the specific combination.

Step 3. Let us focus, now, on the calculation of the relative phase depending on the detector configuration. Each $c_m^\dagger$ gives an i phase term to $|0\rangle^{\otimes N}$, while each $d_m^\dagger$ gives an i phase term to $|1\rangle^{\otimes N}$. Therefore, the states generated by the measurement are of the form

$$\frac{1}{\sqrt{2}}[i^{N-m}|0\rangle^{\otimes N} + i^m|1\rangle^{\otimes N}], \quad (16)$$

with $m \in [0, N-1]$. The set of states given by Eq. (16) is composed of only two states, up to global phases, i.e.,

$$\frac{1}{\sqrt{2}}[i^N|0\rangle^{\otimes N} + |1\rangle^{\otimes N}] \quad \text{and} \quad \frac{1}{\sqrt{2}}[i^N|0\rangle^{\otimes N} - |1\rangle^{\otimes N}].$$

Each state recurs the same number of times. Therefore, we have only two final states, each one arising from 2^{N-1} configurations each. Per each final GHZ-like state the total probability is, then,

$$P_{\mathrm{succ}}^{\mathrm{Tot}} = 2^{1-2N}2^{N-1}\eta^N = 2^{-N}\eta^N, \quad (17)$$

which is the maximal probability of success that we can achieve. The envisioned protocol generates, thus, two GHZ-like states, each one with a $P_{\mathrm{succ}}^{\mathrm{Tot}}$ that in the ideal case is 2^{-N}. This probability corresponds to the success probability for a GHZ projector.

With this the proof is complete. As a last remark, since depending on which detectors click there are two different GHZ-like states, one can gain an extra factor 2 in the total success probability for some applications.

IV. PERFORMANCE

In this section, we give some estimates of the performance of our protocol. Since NV centers are promising candidates for quantum information tasks [36], we consider values [37] of the involved quantities suitable for this system. Let us remind you that for NV centers the photonic qubits can be encoded in time-bin. The quantity that can be compared between different protocols is the entanglement generation rate. The expression of the generation rate r_{GHZ} for GHZ states is

$$r_{\mathrm{GHZ}} = \frac{P_{\mathrm{succ}}^{\mathrm{Tot}}}{t^{\mathrm{Tot}}}, \quad (18)$$

where $P_{\mathrm{succ}}^{\mathrm{Tot}}$ is given by Eq. (17), and t^{Tot} is the total time for each protocol trial. Hence, two factors influence the generation rate, namely the overall transmission η [see Eq. (17)] and the time necessary to perform each task involved in the protocol. Let us focus on deriving t^{Tot}. It is given by the sum of three quantities, i.e., the time necessary to generate all the spin-photon pairs, the time necessary for the photons to travel half the distance between two nodes, and the time necessary for communicating to each node the outcome of the measurements.

(a)

2nd round   1st round

$|l\rangle$ $|e\rangle$

$|l\rangle$ $|e\rangle$

$|a\rangle$ $|a\rangle$

3rd round

(b)

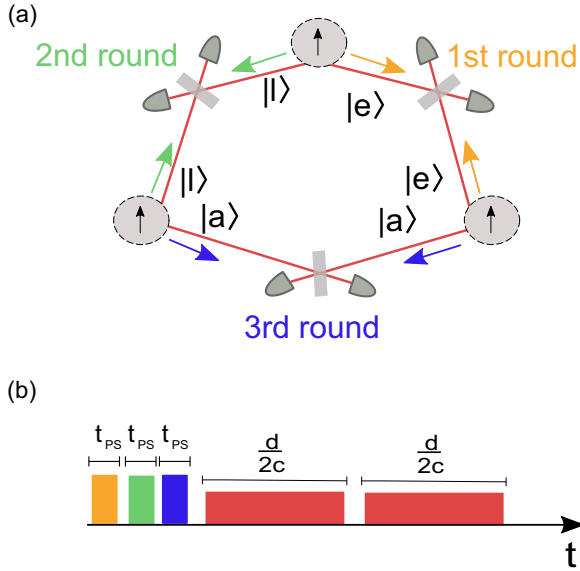t_{PS} t_{PS} t_{PS} $\dfrac{d}{2c}$ $\dfrac{d}{2c}$

t

FIG. 6. Bell measurement synchronization. (a) Three-nodes protocol. In the figure the scheme in the case of three nodes as an example of an odd number of nodes is represented. For an odd number of nodes it is necessary to perform three rounds for generating all the spin-photon pairs: early, late, and "asynchronous." (b) Temporal scheme showing the time line for an odd number of nodes. Three rounds are necessary for generating all the spin-photon pairs. Afterwards, the photons have to travel half d to reach the measurement station. Finally, the nodes have to wait till when the communication of the Bell measurement outcome comes back.

For the sake of simplicity, for odd nodes the generated qubit pairs are $\frac{1}{\sqrt{2}}(|0e\rangle + |1l\rangle)_{AB}$, while for even nodes the generated qubit pairs are $\frac{1}{\sqrt{2}}(|0l\rangle + |1e\rangle)_{AB}$, where $|e\rangle_B$ ($|l\rangle_B$) is an early (late) photon. The expression for the photon-spin generation time has a different expression depending whether the number of nodes is odd or even. Indeed, in the case of an even number, each early (late) mode is coupled with another
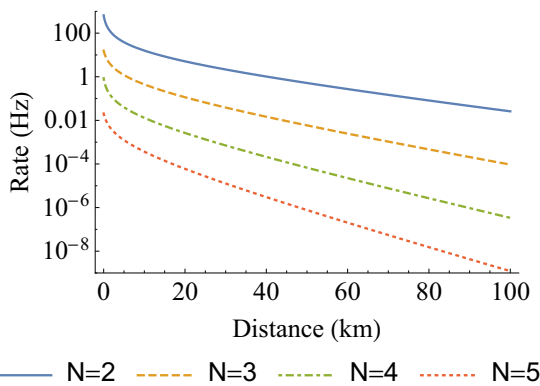

FIG. 7. GHZ generation rate r_{GHZ}. In the figure the generation rate for different values of N (2, 3, 4, and 5) is plotted as a function of the distance d. The values of the experimental parameters are $L_0 = 20$ km, $\eta_{BS} = 10^{-0.03}$ [38], $\eta_D = 0.86$ [39], $p_{fc} = 0.3$, $p_{out} = 0.3$, and $c = 0.2 \times 10^6$ km/s. The total time t^{Tot} for each attempt is given by Eqs. (19) and (20).
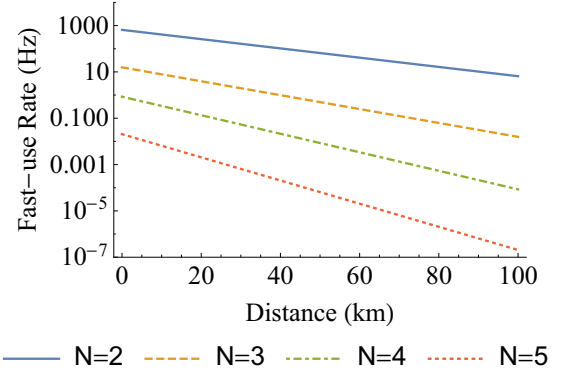

FIG. 8. Fast-use GHZ rate r_{GHZ}. In the figure the fast-use GHZ rate for different values of N (2, 3, 4, and 5) is plotted as a function of the distance d. The values of the experimental parameters are $L_0 = 20$ km, $\eta_{BS} = 10^{-0.03}$ [38], $\eta_D = 0.86$ [39], $p_{fc} = 0.3$, $p_{out} = 0.3$, and $c = 0.2 \times 10^6$ km/s. The total time t^{Tot} is given only by the spin-photon pair preparation time.

early (late) mode. On the contrary, in the case of an odd number of nodes, in order to close the circle (see Fig. 5), there will be one branch, an "asynchronous" branch, where an early mode would be coupled with a late mode (see Fig. 6). This means that in the case of an even number it is sufficient to consider only two rounds (early and late mode) of photon generation per trial, while in the odd case we consider a third round for the "asynchronous branch."

Let us define the time necessary to generate one photon-spin pair as t_{PS}. For the sake of simplicity, we consider that the distance d between two neighboring nodes is fixed. Given the speed of light in an optical fiber c, the total generation time for an even number of nodes is, then,

$$t^{Tot}_{even} = 2t_{PS} + \frac{d}{2c} + \frac{d}{2c}, \tag{19}$$

while for an odd number it is

$$t^{Tot}_{odd} = 3t_{PS} + \frac{d}{2c} + \frac{d}{2c}. \tag{20}$$

Note that there is a factor 2, given by the fact that the photons have to travel only half the distance between the nodes in order to reach the Bell measurement station. Note also that the second $\frac{d}{2c}$ factor is due to the classical communication that has to be transmitted from the measurement stations to the nodes. Note also that there are some applications for which it is not necessary to wait for the measurement and the arrival of the communication of the outcome. In these cases the measurements on the nodes can be realized straight away after the photonic qubits have been sent to the Bell measurement stations, and the results are kept (discarded) after the communication of the success (failure) of the set of Bell measurements. As a consequence, the total time t^{Tot} can be written for this case as just the spin-photon pairs preparation time. We call this rate the fast-use GHZ rate. Concerning the overall transmission η, it is given by the formula [37]

$$\eta = \eta_{BS}\eta_D p_{fc} p_{out} 10^{-\frac{\alpha d}{L_0}}, \tag{21}$$

where L_0 is the attenuation length of the fibers, $\alpha = 0.2$ dB/km, p_{fc} is the frequency conversion efficiency, p_{out}

is the NV outcoupling efficiency, and η_{BS} and η_D are the beam splitter and detector efficiencies, respectively. In Figs. 7 and 8, we present the results for the rate as a function of the distance between two nodes for $N = 2, 3, 4,$ and 5. In Fig. 7 there are the plots for the case t^{Tot}, which is given by Eqs. (19) and (20), while in Fig. 8 the plots are made for t^{Tot} only equal to the spin-photon preparation time. As one might expect from Eq. (17), the curves decrease one term $\frac{\eta}{2}$ per each added node. However, while in Fig. 7 the curves are proportional to $d^{-1}10^{-\frac{\alpha N d}{L_0}}$, in Fig. 8 they are proportional only to the exponential term $10^{-\frac{\alpha N d}{L_0}}$. This results in an improvement of 2 orders of magnitude more in the second case for $d = 100$ km.

V. CONCLUSION

The protocol that we have presented here is an adaptation for matter systems and an arbitrary number of nodes of a protocol [29] meant for fully optical systems and only three parties. We consider the protocol interesting for several reasons. First, it is a natural extension for N nodes of the well-known Barrett-Kok scheme [22,23] and so it is particularly suited for achieving high fidelities. Second, we have proven that in the ideal case, i.e., in the case of no loss, the success probability is optimal. This is, indeed, quite surprising since the scheme is based only on linear optics. Nonetheless, there are some aspects that deserve some attention. Indeed, in a real scenario all the causes of loss and noise have to be taken into account. Unfortunately, optimizing a scheme in a real scenario, where such kinds of processes are involved, is a challenging task. However, it seems to us that the required resources and causes of decoherence and depolarization in our case are minimal. Thus, the protocol is likely optimal also when losses and noise occur. Our scheme presents two intrinsic drawbacks, in that it can only be implemented between nearby nodes and the performance showed in the previous section is quite low. It is, then, of interest to evaluate other protocols that combine distillation procedures with Bell measurements. In this case the parameter of reference would be the generation rate and not anymore the success probability. However, all these protocols would intrinsically be affected by decoherence that would inevitably lower the fidelity. They are not, then, competitive in the high-fidelity regime that we have explored in this article. It is still interesting to investigate if procedures exist for both nearby and distant nodes that allow appealing trade-offs between generation rate and final fidelity.

ACKNOWLEDGMENTS

APPENDIX: NUMERICAL OPTIMIZATION

In the main text, we analytically optimize $F p_{succ}$ and show how to experimentally retrieve this value. In this Appendix, we explain how to perform numerical optimizations over POVMs in order to optimize $F p_{succ}$ for arbitrary input states. One can retrieve the previous expressions for $F p_{succ}$ and p_{succ} in terms of a map Λ acting on system B. The expression for $F p_{succ}$ becomes

$$F p_{succ} = \text{Tr}\{[|GHZ\rangle\langle GHZ|_A \otimes (|GHZ\rangle\langle GHZ|\Lambda)_B]$$
$$\times |\Psi_{in}\rangle\langle\Psi_{in}|_{AB}\}, \quad (A1)$$

where we have substituted $\Pi_B^{succ} = (|GHZ\rangle\langle GHZ|\Lambda)_B$, Λ_B being an arbitrary map. In a similar way the success probability p_{succ} takes the following form:

$$p_{succ} = \text{Tr}\{[\mathbb{1}_A \otimes (|GHZ\rangle\langle GHZ|\Lambda)_B]|\Psi_{in}\rangle\langle\Psi_{in}|_{AB}\}. \quad (A2)$$

Our goal is to find the optimal Λ_B, subject to a fixed p_{succ}, such that the product $F p_{succ}$ is maximal.

1. Choi-Jamiolkowski isomorphism

One can realize the previous optimization using the Choi-Jamiolkowski isomorphism. Let us assume to have two system, S and S', of the same dimension $|S|$. Given the positive map $\Lambda_{S'}$, acting on S', the Choi's theorem states that the matrix

$$\tau_{SS'} = \mathbb{1}_S \otimes \Lambda_{S'}(|\Phi^+\rangle_{SS'}), \quad (A3)$$

where $|\Phi^+\rangle_{SS'} = \frac{1}{\sqrt{|S|}}\sum_{m=1}^{|S|}|mm\rangle_{SS'}$ is a maximally entangled state between systems S and S', has the properties

(i) $\tau_{SS'} \geqslant 0$,
(ii) $\text{Tr}(\tau_{SS'}) = 1$, and
(iii) $\tau_S = \text{Tr}_{S'}(\tau_{SS'}) = \frac{\mathbb{1}_S}{|S|}$.

Given the above-listed first two properties, $\tau_{SS'}$ is a density matrix and it is called the Jamiolkowski state.

2. Initial maximally entangled state

In the case of an initial maximally entangled state, for example, $|\Psi_{in}\rangle_{AB} = |\Phi^+\rangle_{AB} = \bigotimes_{j=1}^{N}\frac{1}{\sqrt{2}}(|00\rangle + |11\rangle)_{A_jB_j}$, the map $\mathbb{1}_A \otimes \Lambda_B$ applied to $|\Psi_{in}\rangle_{AB}$ is a Jamiolkowski state; i.e., $\mathbb{1}_A \otimes \Lambda_B(|\Phi^+\rangle_{AB}) = \tau_{AB}$ is a state. The quantities $F p_{succ}$ and p_{succ} can be rewritten in terms of the Jamiolkowski state, i.e.,

$$F p_{succ} = \text{Tr}[(|GHZ\rangle\langle GHZ|_A \otimes |GHZ\rangle\langle GHZ|_B)\tau_{AB}] \quad (A4)$$

and

$$p_{succ} = \text{Tr}[(\mathbb{1}_A \otimes |GHZ\rangle\langle GHZ|_B)\tau_{AB}]. \quad (A5)$$

Hence, the optimization becomes Max $F p_{succ}$ such that

(i) $\tau_{AB} \geqslant 0$,
(ii) $\text{Tr}(\tau_{AB}) = 1$,
(iii) $\tilde{\tau}_A = \text{Tr}_B(\tau_{AB}) = \frac{\mathbb{1}_A}{2^N}$, and
(iv) p_{succ} is fixed.

The first three conditions are equivalent to the ones of Sec. 1, while the last is necessary for deriving $F p_{succ}$ as a function of p_{succ}.

3. Initial nonmaximally entangled state

Consider now the case when the initial state is nonmaximally entangled, for example, $|\Psi_{in}\rangle_{AB} = \bigotimes_{j=1}^{N}(\sqrt{1-\epsilon}|00\rangle + \sqrt{\epsilon}|11\rangle)_{A_jB_j}$. Let us put system S (S') equal to the initial (final) system AB. One can apply the
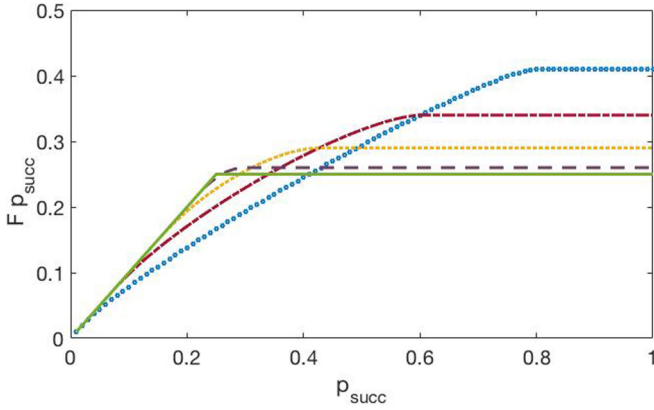
FIG. 9. Numerical optimization of the product $F p_{\text{succ}}$ as a function of p_{succ} for $N = 2$. The curves represent different values of $\epsilon = 0.5, 0.4, 0.3, 0.2$, and 0.1 (solid, dashed, dotted, dot-dashed, and marble curves, respectively).

FIG. 10. Numerical optimization of the product $F p_{\text{succ}}$ as a function of p_{succ} for $N = 3$. The curves represent different values of $\epsilon = 0.5, 0.4, 0.3, 0.2$, and 0.1 (solid, dashed, dotted, dot-dashed, and marble curves, respectively).

Choi-Jamiolkowski isomorphism to $F p_{\text{succ}}$ and p_{succ}. Indeed, we have

$$F p_{\text{succ}} = 2^{2N} \, \text{Tr} \left[|\Psi_{\text{in}}\rangle \langle \Psi_{\text{in}}|_{AB}^{\text{in}} \otimes (|\text{GHZ}\rangle \langle \text{GHZ}|_A \right.$$
$$\left. \otimes |\text{GHZ}\rangle \langle \text{GHZ}|_B)^{\text{fin}} \tilde{\tau}_{AB} \right] \tag{A6}$$

and

$$p_{\text{succ}} = 2^{2N} \, \text{Tr} \left[|\Psi_{\text{in}}\rangle \langle \Psi_{\text{in}}|_{AB}^{\text{in}} \otimes (\mathbb{1}_A \otimes |\text{GHZ}\rangle \langle \text{GHZ}|_B)^{\text{fin}} \tilde{\tau}_{AB} \right],$$
$$\tag{A7}$$

where $\tilde{\tau}_{AB} = \mathbb{1}_{AB}^{\text{in}} \otimes \tau_{AB}^{\text{fin}}$. Here, 2^{2N} is the dimension of one of the two subsystems initial and final. Hence, we want to
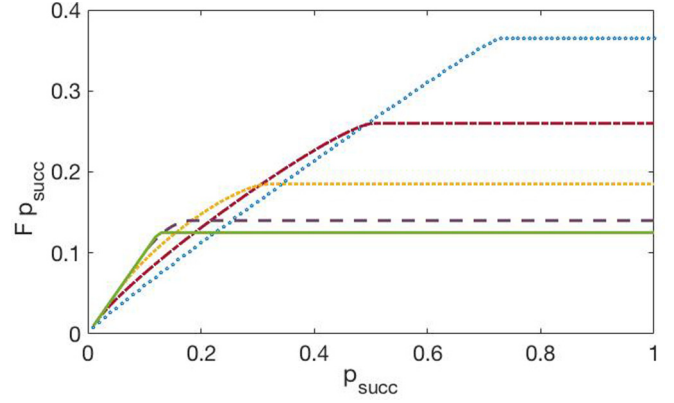
perform the following optimization:

    Max $F p_{\text{succ}}$ such that

  (i) $\tau_{AB}^{\text{fin}} \geqslant 0$,

  (ii) $\text{Tr}(\tau_{AB}^{\text{fin}}) = 1$,

  (iii) $\tilde{\tau}_A^{\text{fin}} = \text{Tr}_B(\tau_{AB}^{\text{fin}}) = \frac{\mathbb{1}_A}{2^N}$, and

  (iv) p_{succ} is fixed.

The above explained optimization has been performed for two and three nodes, providing results in perfect agreement with the analytical upper bounds derived in the main text (Figs. 9 and 10).

[1] A. K. Ekert, Phys. Rev. Lett. **67**, 661 (1991).

[2] S. Pironio, A. Acín, N. Brunner, N. Gisin, S. Massar, and V. Scarani, New J. Phys. **11**, 045021 (2009).

[3] C. H. Bennett, G. Brassard, C. Crépeau, R. Jozsa, A. Peres, and W. K. Wootters, Phys. Rev. Lett. **70**, 1895 (1993).

[4] C. H. Bennett and S. J. Wiesner, Phys. Rev. Lett. **69**, 2881 (1992).

[5] D. Mayers, Phys. Rev. Lett. **78**, 3414 (1997).

[6] N. Aharon, S. Massar, S. Pironio, and J. Silman, New J. Phys. **18**, 025014 (2016).

[7] H. Buhrman, R. Cleve, and W. V. Dam, SIAM J. Comput. **30**, 1829 (2001).

[8] H. Buhrman, R. Cleve, S. Massar, and R. de Wolf, Rev. Mod. Phys. **82**, 665 (2010).

[9] R. Cleve and H. Buhrman, Phys. Rev. A **56**, 1201 (1997).

[10] L. K. Grover, arXiv:quant-ph/9704012.

[11] Y. Li, P. C. Humphreys, G. J. Mendoza, and S. C. Benjamin, Phys. Rev. X **5**, 041007 (2015).

[12] Y. Li and S. C. Benjamin, Phys. Rev. A **94**, 042303 (2016).

[13] M. Hillery, V. Bužek, and A. Berthiaume, Phys. Rev. A **59**, 1829 (1999).

[14] M. Epping, New J. Phys. **19**, 093012 (2017).

[15] M. Christandl and S. Wehner, in *Advances in Cryptology - ASIACRYPT 2005*, edited by B. Roy, Lecture Notes in Computer Science Vol. 3788 (Springer, Berlin, Heidelberg, 2005), https://link.springer.com/chapter/10.1007/11593447_12.

[16] S. Muralidharan, L. Li, J. Kim, N. Lütkenhaus, M. D. Lukin, and L. Jiang, Sci. Rep. **6**, 20463 (2016).

[17] D. Gottesman and I. L. Chuang, Nature (London) **402**, 390 (1999).

[18] S. Muralidharan, J. Kim, N. Lutkenhaus, M. D. Lukin, and L. Jiang, Phys. Rev. Lett. **112**, 250501 (2014).

[19] W. J. Munro, A. M. Stephens, S. J. Devitt, K. A. Harrison, and K. Nemoto, Nat. Photonics **6**, 777 (2012).

[20] P. Kómár, E. M. Kessler, M. Bishof, L. Jiang, A. S. Sørensen, J. Ye, and M. D. Lukin, Nat. Phys. **10**, 582 (2014).

[21] D. M. Greenberger, M. A. Horne, and A. Zeilinger, in *Bell's Theorem, Quantum Theory, and Conceptions of the Universe*, edited by M. Kafatos (Kluwer Academic, Dordrecht, 1989).

[22] S. D. Barrett and P. Kok, Phys. Rev. A **71**, 060310(R) (2005).

[23] Y. L. Lim, A. Beige, and L. C. Kwek, Phys. Rev. Lett. **95**, 030505 (2005).

[24] P. Komar, T. Topcu, E. M. Kessler, A. Derevianko, V. Vuletic, J. Ye, and M. D. Lukin, Phys. Rev. Lett. **117**, 060506 (2016).

[25] N. H. Nickerson, J. F. Fitzsimons, and S. C. Benjamin, Phys. Rev. X **4**, 041041 (2014).

[26] S. Bose, V. Vedral, and P. L. Knight, Phys. Rev. A **57**, 822 (1998).

[27] A. Zeilinger, M. A. Horne, H. Weinfurter, and M. Zukowski, Phys. Rev. Lett. **78**, 3031 (1997).

[28] M. Cuquet and J. Calsamiglia, Phys. Rev. A **86**, 042304 (2012).

[29] M. Zukowski, A. Zeilinger, and H. Weinfurter, Ann. New York Acad. Sci. **755**, 91 (1995).

[30] H. Bernien, B. Hensen, W. Pfaff, G. Koolstra, M. S. Blok, L. Robledo, T. H. Taminiau, M. Markham, D. J. Twitchen, L. Childress, and R. Hanson, Nature (London) **497**, 86 (2013).

[31] W. B. Gao, A. Imamoglu, H. Bernien, and R. Hanson, Nat. Photonics **9**, 363 (2015).

[32] D. Hucul, I. Inlek, G. Vittorini, C. Crocker, S. Debnath, S. Clark, and C. Monroe, Nat. Phys. **11**, 37 (2015).

[33] A. Delteil, Z. Sun, W. B. Gao, E. Togan, and S. Faelt, Nat. Phys. **12**, 218 (2016).

[34] J. Y. Lee, L. Yin, G. P. Agrawal, and P. M. Fauchet, Opt. Express **18**, 11514 (2010).

[35] V. Caprara Vivoli, P. Sekatski, J.-D. Bancal, C. C. W. Lim, B. G. Christensen, A. Martin, R. T. Thew, H. Zbinden, N. Gisin, and N. Sangouard, Phys. Rev. A **91**, 012107 (2015).

[36] B. Hensen, H. Bernien, A. E. Dréau, A. Reiserer, N. Kalb, M. S. Blok, J. Ruitenberg, R. F. L. Vermeulen, R. N. Schouten, C. Abellán, W. Amaya, V. Pruneri, M. W. Mitchell, M. Markham, D. J. Twitchen, D. Elkouss, S. Wehner, T. H. Taminiau, and R. Hanson, Nature (London) **526**, 682 (2015).

[37] S. B. van Dam, P. C. Humphreys, F. Rozpędek, S. Wehner, and R. Hanson, Quantum Sci. Technol. **2**, 034002 (2017).

[38] 50:50, 1064 nm, 2×2 Polarization-Maintaining Fiber Optic Couplers/Taps, Thorlabs.

[39] I. E. Zadeh, J. W. N. Los, R. B. M. Gourgues, G. Bulgarini, S. M. Dobrovolskiy, V. Zwiller, and S. N. Dorenbos, arXiv:1801.06574.